DE GRUYTER
Z. Naturforsch. 2020; 75(1–2)b: 173–181

Eric Sperlich and Martin Köckerling*

Cation-anion pairs of niobium clusters of the type $[Nb_6Cl_{12}(RCN)_6][Nb_6Cl_{18}]$ (R = Et, ^{n}Pr, ^{i}Pr) with nitrile ligands RCN forming stabilizing inter-ionic contacts

https://doi.org/10.1515/znb-2019-0177
Received November 6, 2019; accepted November 28, 2019

Abstract: Three new niobium cluster compounds with edge bridged, octahedral hexanuclear metal cores have been synthesised. They consist of cluster pairs with $[Nb_6Cl_{12}(RCN)_6]^{2+}$ cations, $[Nb_6Cl_{18}]^{2-}$ anions, and co-crystallised nitrile molecules, with $R = C_2H_5$ (propionitrile), $^nC_3H_7$ (butyronitrile), $^iC_3H_7$ (isobutyronitrile). The synthesis is based on the dehydration of $[Nb_6Cl_{14}(H_2O)_4] \cdot 4(H_2O)$ with carboxylic acid anhydrides in the presences of an excess of the respective nitrile. An interesting aspect of these compounds is that the metal atoms of the cluster cation have an average oxidation state different from that of the cluster anion, the former being oxidized losing two electrons. In crystals of all three compounds layers of cluster cations are separated by layers of cluster anions. Perpendicular to these layers of the same cluster types, every cation is surrounded by four anions and vice versa. Between the cations and anions short distances are found between the halogenido ligands and the positively charged C atoms of the nitrile ligands (N–C · · · Cl angles of ~90°). These contacts indicate relatively strong dipole-dipole interactions, which presumably contribute to the arrangement of the cluster ions in the crystals.

Keywords: cluster; crystal structure; dipole-dipole interaction; halide; niobium; nitrile ligand.

Dedicated to: Professor Arndt Simon on the Occasion of his 80th birthday.

1 Introduction

Halides or oxides of early transition metals are often characterized by core units with metal-metal bonds surrounded by shells of halogenido or oxido ligands [1–6]. Many of such cluster compounds with low nuclearity have been described [7–9]. Many compounds are known with hexanuclear metal atom units, M_6, of octahedral shape, which can be either edge-bridged, ($[M_6X^i_{12}]$ type) or face-bridged, ($[M_6X^i_8]$ type) by *inner* ligands X^i. Further *outer* (*außen*) ligands X^a are bonded terminally. These exo-bonded ligands can be exchanged by other ligands by soft solution methods, giving rise to an extensive cluster solution chemistry [10–14]. The solution-made products in most cases contain discrete units. The $[M_6X^i_{12}]$ type clusters of the group 5 metals niobium and tantalum, which carry anionic or neutral ligands X^a, have the formula $[M_6X^i_{12}X^a_6]^n$, with charges n ranging from −4 to +3. These charges are co-determined by the number of electrons in the metal-metal bonding states. If all bonding states are occupied, they carry 16 electrons (CBE's, cluster based electrons or VEC, valence electron concentration) [6, 15, 16]. These cluster units can be oxidised, such that cluster compounds with 15 respectively 14, CBE's are generated [17, 18].

There is also an interesting, but so far very small group of Nb or Ta cluster compounds, which consist of two different cluster units within the same compound (cluster pairs). Reported cases with charged cluster units are the two heteronuclear examples, $[Nb_6Cl_{12}(EtOH)_6][Mo_6X_{14}]$ und $[Ta_6Cl_{12}(EtOH)_6][Mo_6X_{14}]$, ($X$ = Cl, Br) and one homonuclear example, $[Ta_6Cl_{12}(^nPrCN)_6][Ta_6Cl_{18}] \cdot 2(^nPrCN)$ (Et = C_2H_5, $^nPr = C_3H_7$), but one example with neutral cluster units, $[(Ta_6Cl_{12})Cl_3(^nBuCN)_3][(Ta_6Cl_{12})Cl_4(^nBuCN)_2] \cdot (^nBuCN)$ ($^nBu = C_4H_9$) has also been described [19–21].

In this paper we present the first three homonuclear niobium cluster pair compounds of compositions $[Nb_6Cl_{12}(RCN)_6][Nb_6Cl_{18}] \cdot 2(RCN)$, with $R = C_2H_5$ (propionitrile), **1**, $R = {}^nC_3H_7$ (^{n}butyronitrile), **2**, and $R = {}^iC_3H_7$ (^{i}butyronitrile), **3**.

2 Results and discussion

The synthesis of the new compounds **1–3** is based on dehydration reactions of $[Nb_6Cl_{14}(H_2O)_4] \cdot 4(H_2O)$ with carboxylic acid anhydrides (acetic anhydride, Ac_2O, for **1** and **3**, trimethylacetic anhydride, $TMAc_2O$, for **2**) in solutions of

---

***Corresponding author: Martin Köckerling,** Institute of Chemistry, Solid-State Inorganic Chemistry Group, University of Rostock, Albert-Einstein-Straße 3a, 18059 Rostock, Germany; and University of Rostock, Department Life, Light and Matter, 18051 Rostock, Germany, Fax: +49 381 498 6382, E-mail: martin.koeckerling@uni-rostock.de
Eric Sperlich: Institute of Chemistry, Solid-State Inorganic Chemistry Group, University of Rostock, Albert-Einstein-Straße 3a, 18059 Rostock, Germany

the respective nitriles. The reaction vessels were stored at elevated temperature (40°C for **1**) for 2 days and then for one further week at room temperature. Scheme 1 shows the equation of the synthesis of **1**.

According to this scheme the formation of the title cluster compounds requires extra chloride ions, which are not supplied with the starting materials. As mentioned in several previous papers, it is assumed that cluster decomposition happens in solution, possibly in disproportionation reactions, supplying thereby halide ions. Such disproportionation reactions are assumed to be accelerated by the presence of water, oxygen (air) or induced by elevated temperatures [22–26]. Whereas the tantalum cluster pair compound $[Ta_6Cl_{12}(^nPrCN)_6][Ta_6Cl_{18}] \cdot 2(^nPrCN)$ described in the literature was produced at elevated temperatures under air with a reaction time of more than 6 months in low yield, we assume that in the case of the reaction protocol for **1–3** the strong acidic reaction conditions lead to a quick oxidative degradation of clusters supplying the chloride ions needed for the formation of the title compounds much more quickly [20]. This assumption is supported by the fact that the anion $[Nb_6Cl_{18}]^{2-}$ comprises a cluster deprived of two electrons with respect to the starting material. For the formation of the title compounds several chemical transformations must happen either simultaneously or step-by-step. These include the dehydration of the starting cluster compound, the mentioned side reaction of cluster decomposition and formation of Cl^- ions, the formation of the $[Nb_6Cl_{18}]^{n-}$ units and their oxidation, and the ligand exchange reaction leading to the $[Nb_6Cl_{12}(RCN)_6]^{2+}$ cations. Unfortunately, so far no information on details of the mechanism can be offered. The compounds **1** and **2** were obtained in yields of 50 and 70%, respectively, whereas of **3** only a few crystals could be obtained. The decomposition of one cluster unit of the starting material gives a maximum of 14 chloride ions, which allows for 7 cluster pairs to form. For this redistribution of ligands, the maximum yield could be 93%, which is not reached. However, the deep colour of the reaction mixtures, which still exists after the crystallization of the reaction products, suggests the presence of more and other cluster compounds in solution.

The cluster pair compound **1** crystallises in the monoclinic space group $P2_1/c$ while **2** and **3** crystallise in the triclinic space group $P\bar{1}$. The latter ones are isotypic to the known compound $[Ta_6Cl_{12}(^nPrCN)_6][Ta_6Cl_{18}] \cdot 2(^nPrCN)$ [20]. Table 1 lists the crystallographic data of the title compounds and Table 2 presents average values and ranges of selected interatomic distances within the cluster units.

Both, the cluster cations $[Nb_6Cl_{12}(RCN)_6]^{2+}$ with $R =$ Et, ^{n}Pr and ^{i}Pr and the cluster anions $[Nb_6Cl_{18}]^{2-}$ contain the ubiquitous, edge-bridged octahedral $[Nb_6Cl^i_{12}]$ unit, but with different oxidation states. The cluster cations contain 16 CBE's, whereas the cluster anions are two-electron oxidised species with 14 CBE's. Figure 1 shows the molecular structures of the cluster cations in **1–3** and, as one example, the cluster anion as found in **1**. The existence of cluster compounds with the metal atoms exhibiting two different oxidation states is quite uncommon. One further example beside the above mentioned Nb and Ta double cluster compounds is the zirconium cluster double salt $Cs[ZrCl_5] \cdot Cs_2[(Zr_6Z)X_{15}]$ ($Z =$ B or Mn; $X =$ Cl or Cl + I) [27, 28].

The assignment of the two different oxidation states of the cluster units in the title compounds is supported by the Nb–Nb and Nb–Cl^i distances (see Table 2). In the cluster anions (oxidized units) the Nb–Nb distances are longer by ~0.12 Å than those in the 16 CBE-cations; **1**: 3.0282 Å, **2**: 3.0353 Å, **3**: 3.0293 Å, compared to **1**: 2.9076 Å, **2**: 2.9092 Å, and **3**: 2.9098 Å. At the same time the Nb–Cl^i distances are slightly longer in the oxidized units than in the cluster units with 16 CBE's. These observations are related to the number of electrons present in the HOMO of the cluster units, which has a_{2u} symmetry and is metal–metal bonding for 16 and 15 CBEs and (slightly) metal–X^i antibonding in character [6, 15, 16]. Comparable bonding situations/interatomic distances are described for example for the compounds $A^I_2[Nb_6Cl_{18}]$ with $A^I =$ singly-charged organic cation, $K_4[Nb_6Cl_{18}]$, and others [29, 30]. All the other interatomic distances assigned to chemical bonds are found in their expected ranges.

Figures 2 and 3 show the arrangement of cluster units of **1** and (exemplarily) of **3** in a plot of 2×1×2 respectively 2×2×2, neighbouring unit cells. For **3** two different viewing directions are shown, along the crystallographic *a* (Fig. 3, left) and *b* (Fig. 3, right) directions. In both Figures the metal atom octahedra of the cluster cations are shown in a different colour than the Nb_6 units of the anion. It is evident that in both structures layers of cluster cations are separated by layers of cluster anions.

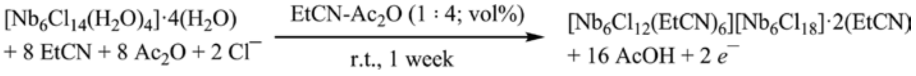

$$[Nb_6Cl_{14}(H_2O)_4] \cdot 4(H_2O) + 8\ EtCN + 8\ Ac_2O + 2\ Cl^- \xrightarrow[\text{r.t., 1 week}]{EtCN\text{-}Ac_2O\ (1:4;\ vol\%)} [Nb_6Cl_{12}(EtCN)_6][Nb_6Cl_{18}] \cdot 2(EtCN) + 16\ AcOH + 2\ e^-$$

Scheme 1: Reaction scheme for the formation of the cluster pair compounds, exemplarily for **1**.

Table 1: Crystal data, data collection and structure refinement parameters for **1–3**.

Compound	1	2	3
Formula	$C_{24}H_{40}Cl_{30}N_8Nb_{12}$	$C_{32}H_{56}Cl_{30}N_8Nb_{12}$	$C_{32}H_{56}Cl_{30}N_8Nb_{12}$
M_r	2619.09	2731.31	2731.26
Cryst. size, mm³	0.5 × 0.1 × 0.1	0.3 × 0.2 × 0.04	0.8 × 0.3 × 0.3
T, K	123	123	123
Crystal system	Monoclinic	Triclinic	Triclinic
Space group; Z	$P2_1/c$; 2	$P\bar{1}$; 1	$P\bar{1}$; 1
a, Å	13.1769(4)	12.1579(6)	11.4039(9)
b, Å	21.5853(6)	12.5867(6)	12.997(1)
c, Å	12.5221(4)	13.1617(6)	13.576(1)
α, deg	90	93.853(2)	97.242(2)
β, deg	94.746(1)	93.886(2)	92.288(2)
γ, deg	90	93.501(2)	91.041(2)
V, Å³	3549.4(2)	2000.6(2)	1994.0(3)
D_{calcd}, g cm^{-3}	2.45	2.27	2.27
μ(Mo$K\alpha$), cm^{-1}	29.8	26.5	26.6
F(000), e	2484	1306	1306
hkl range	±20, ±33, ±19	±18, ±18, ±19	±15, ±17, ±18
$2\theta_{max}$, deg	66.6	64.2	58.4
$(\sin\theta/\lambda)_{max}$, Å^{-1}	0.772	0.748	0.685
Refl. measured	325014	107615	49309
Refl. unique/R_{int}	13617/0.035	13983/0.049	10672/0.027
Param. refined	339	375	378
$R(F)^a/wR(F^2)^b$ [$I > 2\,\sigma(I)$]	0.0169/0.0362	0.0273/0.0504	0.0347/0.0779
$R(F)^a/wR(F^2)^b$ (all refl.)	0.0190/0.0369	0.0415/0.0549	0.0445/0.0856
GoF $(F^2)^c$	1.128	1.034	1.161
$\Delta\rho_{fin}$ (max/min), e Å^{-3}	0.80/ − 0.47	1.71/ − 1.00	1.69/ − 0.95

$^aR(F) = \Sigma||F_o| - |F_c||/\Sigma|F_o|$; $^b wR(F^2) = [\Sigma w(F_o^2 - F_c^2)^2/\Sigma w(F_o^2)^2]^{1/2}$, $w = [\sigma^2(F_o^2) + (AP)^2 + BP]^{-1}$, where $P = (\text{Max}(F_o^2, 0) + 2F_c^2)/3$;
$^c\text{GoF} = S = [\Sigma w(F_o^2 - F_c^2)^2/(n_{obs} - n_{param})]^{1/2}$.

Table 2: Ranges and average values of selected interatomic distances (Å) within the cluster units of **1–3** and $[Ta_6Cl_{12}(^nPrCN)_6][Ta_6Cl_{18}]$ [20].

	Cluster cation		Cluster anion	
	Range (Å)	**Av. (Å)**	**Range (Å)**	**Av. (Å)**
$[Nb_6Cl_{12}(EtCN)_6][Nb_6Cl_{18}]$ (**1**)				
Nb–Nb	2.8984(2)–2.9157(2)	2.9076	3.0182(2)–3.0348(2)	3.0282
Nb–Cl^i	2.4421(3)–2.4626(3)	2.4535	2.4242(3)–2.4317(3)	2.4278
Nb–Cl^a	–	–	2.4544(4)–2.4944(3)	2.4809
Nb–N	2.262(1)–2.279(1)	2.268	–	–
$[Nb_6Cl_{12}(^nPrCN)_6][Nb_6Cl_{18}]$ (**2**)				
Nb–Nb	2.9023(3)–2.9201(3)	2.9092	3.0232(3)–3.0458(3)	3.0353
Nb–Cl^i	2.4443(6)–2.4665(6)	2.4557	2.4182(6)–2.4393(6)	2.4300
Nb–Cl^a	–	–	2.4618(6)–2.4964(6)	2.4832
Nb–N	2.266(2)–2.275(2)	2.270	–	–
$[Nb_6Cl_{12}(^iPrCN)_6][Nb_6Cl_{18}]$ (**3**)				
Nb–Nb	2.9030(5)–2.9221(5)	2.9098	3.0170(5)–3.0417(5)	3.0293
Nb–Cl^i	2.444(1)–2.467(1)	2.4537	2.414(1)–2.437(1)	2.427
Nb–Cl^a	–	–	2.476(1)–2.480(1)	2.479
Nb–N	2.264(3)–2.270(3)	2.27	–	–
$[Ta_6Cl_{12}(^nPrCN)_6][Ta_6Cl_{18}]$				
Ta–Ta	2.8627(4)–2.8795(4)	2.87	2.9742(4)–2.9903(5)	2.9815
Ta–Cl^i	2.4506(17)–2.4700(18)	2.4584	2.4162(19)–2.440(2)	2.4304
Ta–Cl^a	–	–	2.4672(19)–2.499(2)	2.4871
Ta–N	2.245(7)–2.264(7)	2.253	–	–

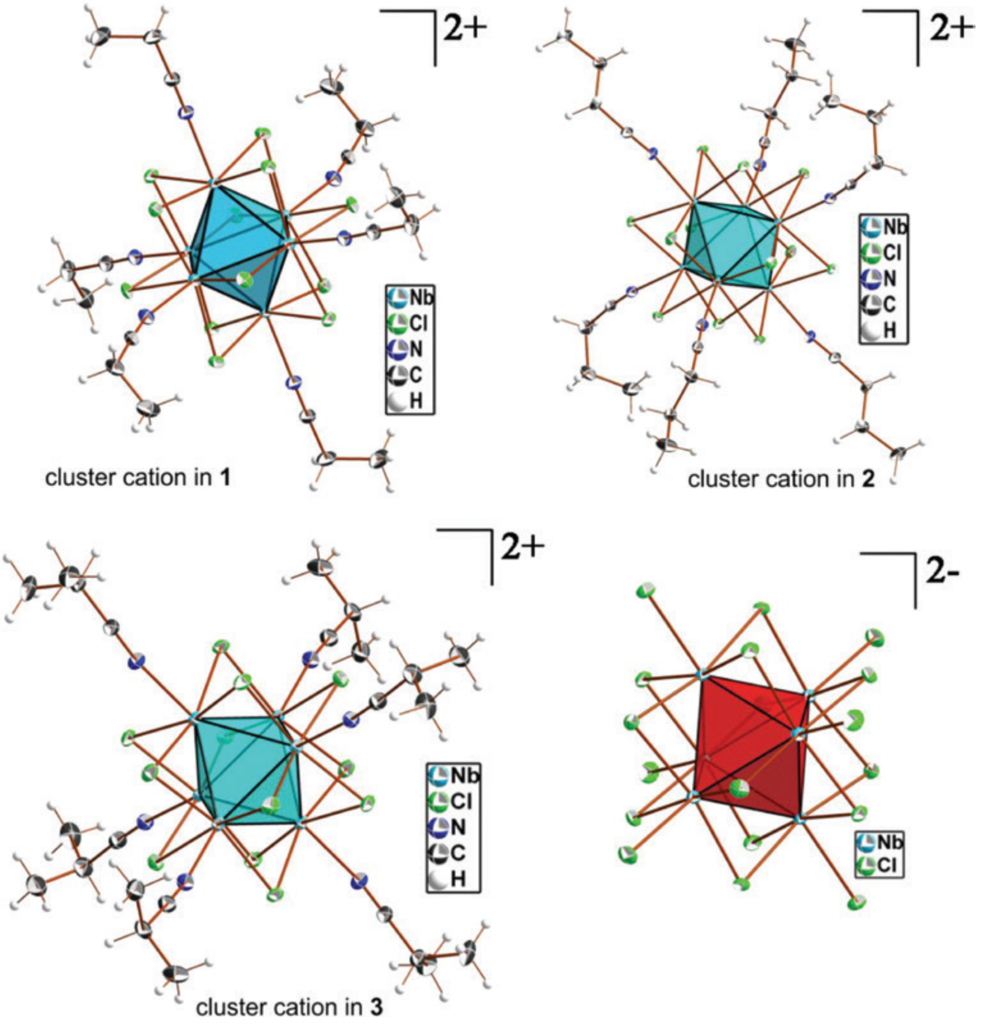

Fig. 1: The molecular structures of the $[Nb_6(RCN)_6]^{2+}$ cluster cations of **1–3** and the $[Nb_6Cl_{18}]^{2-}$ anion exemplarily, as found in **1**. Displacement ellipsoids are drawn at the 50% probability level. Niobium atom octahedra are in drawn in a polyhedral representation, with blue colour for the cluster cations and red for the anions.

For **1** this happens in the crystallographic *a* direction and for **2** and **3** (and for $[Ta_6Cl_{12}(^nPrCN)_6][Ta_6Cl_{18}] \cdot 2(^nPrCN)$ [20]) in both the *b* and *c* direction. Idealizing this cluster arrangements by assuming the presence of identical, neutral cluster units with same orientations, the structure of **1** could be derived from a cubic face-centred structure whereas **2** and **3** from a *C*-centered structure.

In both structures every cluster cation is not surrounded by the usual six neighbours, but only by four nearest neighbour anions and vice versa, every cluster anion by four cations. This structural arrangement is perhaps supported by a special type of interactions, found for the first time with niobium cluster compounds, i.e. halogen dipole-dipole interactions. Figure 4 shows for **1** that the $[Nb_6Cl_{18}]^{2-}$ anions are arranged around the cluster cation, such that negatively charged chlorido ligands of the cluster anions, or the N atoms of the co-crystallised nitrile molecules, have short distances to the positively charged C atoms of the nitrile groups ($C^{nitrile}$) of neighbouring cluster cations, with ~90° angles between the almost linear –NC*R* groups and the Cl–Nb bonds. The $Cl \cdots C^{nitrile}$ interactions in **1** with distances <4 Å are numbered and shown in Fig. 4 as blue dashed lines. For **2**, **3** and (for comparison) for $[Ta_6Cl_{12}(^nPrCN)_6][Ta_6Cl_{18}]$ [20] this orientation is shown in Fig. 5. The numerical values as well as their $N–C \cdots Cl$ angles are listed in Table 3.

As is shown in Fig. 4 (left), each cluster cation of **1** exhibit three symmetry-independent $Cl \cdots C^{nitrile}$ contacts. Their number increases to a total of six contacts because of the inversion symmetry of the structure and the cluster units. The corresponding scheme of interactions exists for the environment of the cluster anion, as shown in Fig. 4

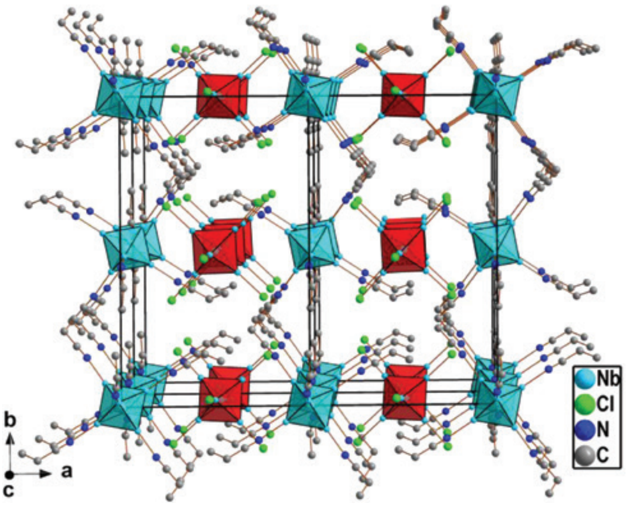

Fig. 2: The arrangement of cluster ions in crystals of **1** in a view of four unit cells along *c* showing the arrangement of cations and anions in layers. The Nb atom octahedra of the cations are shown as blue polyhedra and of the anions as red polyhedra.

(middle). Two further $Cl\cdots C^{nitrile}$ interactions are found between Cl^{i} atoms of the cluster anion and the $C^{nitrile}$ atoms of the co-crystallised EtCN molecules, Fig. 4 (right). All these contacts are located within the *ac* layer of the unit cell (stacked along *b*), such that a layered structure exists without bonding interaction between the layers, as seen in Fig. 3 (right).

In **2** also five independent $Cl\cdots C^{nitrile}$ interactions exist (within distances <4 Å). But here, they all exist between the cluster cations and anions, see Fig. 5 (left). This is exactly the same situation as in the literature-known Ta cluster complex [20]. $[Ta_6Cl_{12}(^{n}PrCN)_6][Ta_6Cl_{18}]\cdot 2(^{n}PrCN)$ which is isostructural with **2**. In **3** the environment of the *iso*-propyl nitrile ligands allow only for three independent contacts, see Fig. 5 (middle). In **2** and **3** these bonding interactions are located within the *bc* layers, which are stacked without interactions along *a*, as shown in Fig. 3 (right).

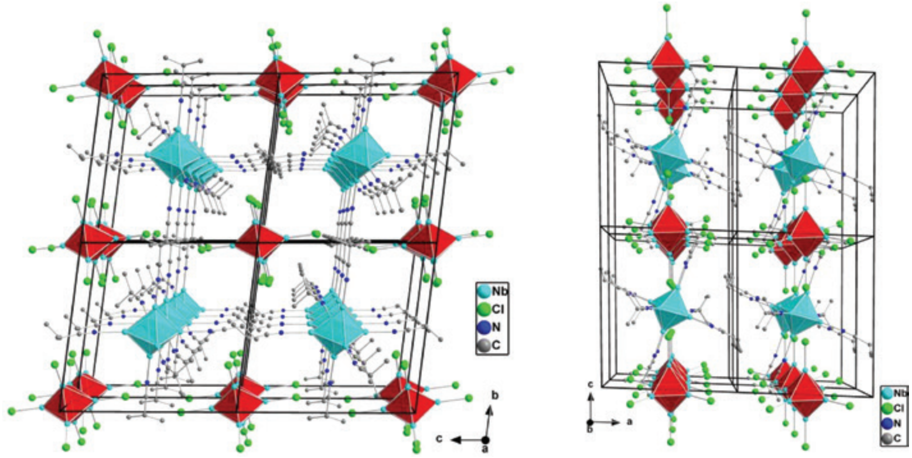

Fig. 3: The arrangement of cluster ions in crystals of **3** in views of eight unit cells along *a* (left) and *b* (right) showing the arrangement of cations and anions in layers. The Nb atom octahedra of the cations are shown as blue polyhedra and of the anions as red polyhedra.

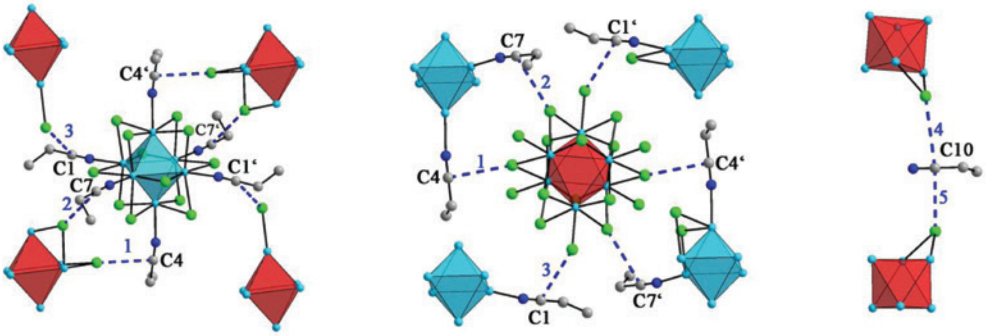

Fig. 4: View of the environments of cluster cation (left) and cluster anion (middle and right) in the structure of **1** with $C^{nitrile}\cdots Cl$ contacts being numbered and shown as blue dotted lines.

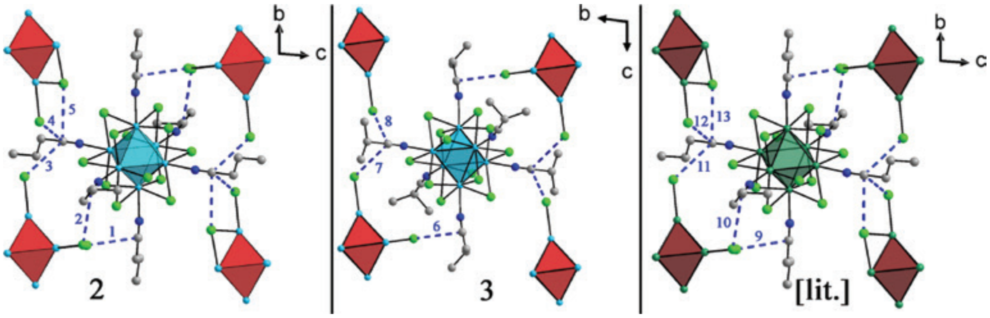

Fig. 5: Cluster cation environments in **2**, **3** and $[Ta_6Cl_{12}(PrCN)_6][Ta_6Cl_{18}]$ with $C^{nitrile}\cdots Cl$ contacts labelled as blue dotted lines.

Table 3: Interatomic distances and angles of the $C^{nitile}\cdots Cl$ dipole-dipole interactions in **1–3** and $[Ta_6Cl_{12}(PrCN)_6][Ta_6Cl_{18}]$.

$[Nb_6Cl_{12}(EtCN)_6][Nb_6Cl_{18}]$ (1)			$[Nb_6Cl_{12}(^nPrCN)_6][Nb_6Cl_{18}]$ (2)			$[Nb_6Cl_{12}(^iPrCN)_6][Nb_6Cl_{18}]$ (3)		
Contact	$C^{nitile}\cdots Cl$ distance (Å)	$N–C\cdots Cl$ angle (deg)	Contact	$C^{nitile}\cdots Cl$ distance (Å)	$N–C\cdots Cl$ angle (deg)	Contact	$C^{nitile}\cdots Cl$ distance (Å)	$N–C\cdots Cl$ angle (deg)
1	3.51	86	1	3.52	91	6	3.64	91
2	3.59	92	2	3.73	99	7	3.73	109
3	3.33	96	3	3.70	109	8	3.37	98
4	3.93	86	4	3.29	98			
5	3.50	87	5	3.69	91			

$[Ta_6Cl_{12}(^nPrCN)_6][Ta_6Cl_{18}]$ [20]		
Contact	$C^{nitile}\cdots Cl$ distance (Å)	$N–C\cdots Cl$ angle (deg)
9	3.55	92
10	3.75	100
11	3.72	110
12	3.30	99
13	3.67	91

Numbering of contacts as in Figs. 4 and 5.

Halogen $\cdots C^{nitrile}$ dipole-dipole interactions have been described for other nitrile containing compounds and seem to contribute significantly to the Gibbs free energy of crystalline compounds [31].

The compounds **1** and **2** were further characterized by elemental analyses. Of compound **3** no reliable data are available (so far), because of the low yield and the small amount of material.

The nitrile coordination in **1–3** is besides the structural evidence also recognized by the shifts of the $C\equiv N$ stretching frequencies in the IR spectra. The values are found at 2277 cm^{-1} (**1**), 2281 cm^{-1} (**2**) and 2275 cm^{-1} (**3**). Compared to the corresponding frequencies of the free ligands RCN (2262 cm^{-1} for $R = C_2H_5$, 2260 cm^{-1} for $R = {}^nC_3H_7$, and 2255 cm^{-1} for $R = {}^iC_3H_7$ [32]), the frequencies in the cluster complexes are shifted to higher values by 15–21 cm^{-1}. Such frequency shifts are often observed when nitriles are coordinated at metal atoms and are explained by increased σ bond strengths [33]. Comparable values of $C\equiv N$ stretching modes are found for cluster complexes of the type $[Nb_6Cl_{14}(RCN)_4]$ for $R = C_2H_5$, ${}^nC_3H_7$, and ${}^nC_4H_9$ [34].

^1H NMR spectra were recorded of all three title compounds in [D6]DMSO. Unfortunately, the DMSO molecules substitute the nitrile ligands, such that the NMR data contain besides others only the signals of the free, non-coordinated nitrile ligands. Nevertheless, the values are given in the Experimental section.

3 Conclusion

The syntheses and single-crystal structures of three new niobium cluster compounds are presented. They belong to the so far very small group of hexanuclear cluster compounds, which comprise two different cluster units within the same compound, i.e. cluster pairs. The cluster cations and cluster anions are arranged in the in layers. Between the C atoms of nitrile groups of the cluster cations and Cl atoms of the cluster anions halogen $\cdots$ C$^{\text{nitrile}}$ interactions are observed.

4 Experimental section

4.1 General

IR spectra were recorded in the range of 4000–500 cm^{-1} with a Bruker Alpha FT-IR spectrometer with an ATR device on samples of 1–3, which were exposed to high vacuum to remove the co-crystallised nitrile molecules. Elemental analyses were obtained with a Flash Thermo Quest and a micro analyser for C/H/N/S TruSpec-932 from Leco GmbH, Germany. The ^{1}H NMR spectroscopic data was collected with a Bruker AVANCE 250 or a Bruker AVANCE 300 instrument.

4.2 Synthesis

All reactions were carried out in air. The solvents were used without drying as they were obtained commercially. The dehydration reactions were carried out analogously to the previously reported procedure [13, 30]. Microscopic view of crystals of the title compounds are given in Figs. 6–8.

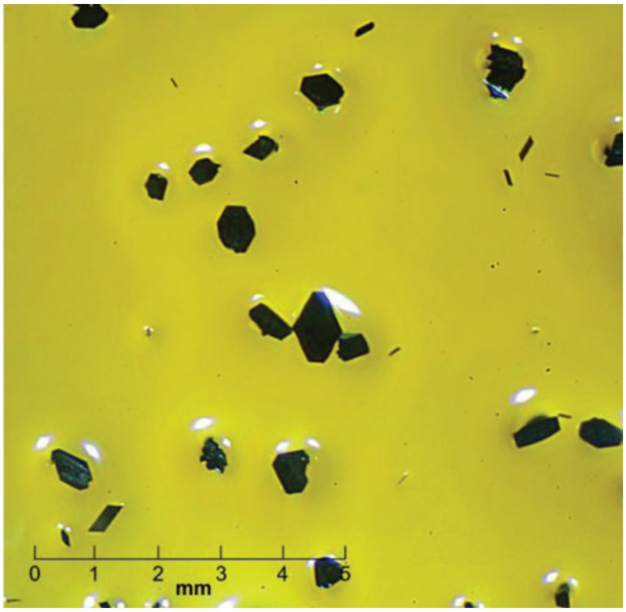

Fig. 6: Light-microscopic view of crystals of [Nb$_6$Cl$_{12}$(EtCN)$_6$][Nb$_6$Cl$_{18}$] · 2(EtCN) (**1**) (20 times magnification).

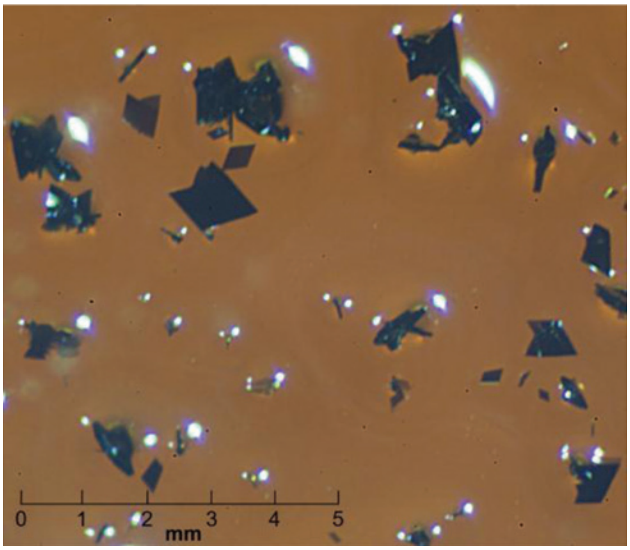

Fig. 7: Light-microscopic view of crystals of [Nb$_6$Cl$_{12}$(^{n}PrCN)$_6$][Nb$_6$Cl$_{18}$] · 2(^{n}PrCN) (**2**) (20 times magnification).

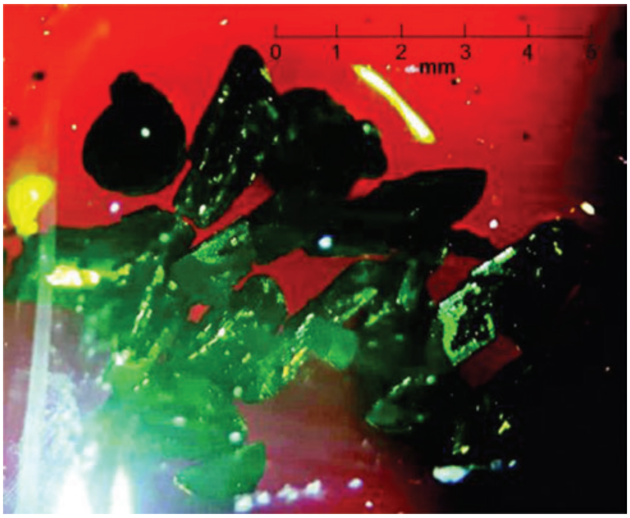

Fig. 8: Light-microscopic view of crystals of [Nb$_6$Cl$_{12}$(^{i}PrCN)$_6$][Nb$_6$Cl$_{18}$] · 2 (^{i}PrCN) (**3**) (20 times magnification).

4.2.1 [Nb$_6$Cl$_{14}$(H$_2$O)$_4$] · 4(H$_2$O)

The preparation of this starting compound was carried out as described in the literature [35]. The cluster compound K$_4$[Nb$_6$Cl$_{18}$] was dissolved in bi-distilled water, stirred for 24 h, and then the product was precipitated with concentrated HCl. The resulting black solid was washed with HCl, followed by drying at $T = 60°\text{C}$ to give $[Nb_6Cl_{14}(H_2O)_4] \cdot 4(H_2O)$ in good yield.

4.2.2 $[Nb_6Cl_{12}(EtCN)_6][Nb_6Cl_{18}] \cdot 2(EtCN)$ (1)

A glass vial with screw cap was filled with 50 mg (41.74 µmol) of the precursor compound $[Nb_6Cl_{14}(H_2O)_4] \cdot 4(H_2O)$ and 5 mL of a mixture of propionitrile (EtCN) and acetic anhydride (Ac_2O) in the volume ratio of 1:4. The glass was closed and heated at 40°C for 2 days. Then, it was stored for several days at room temperature, resulting in the precipitation of black crystals of the title compound **1**. The crystallization continues for a longer period of time, such that the solution is still dark in color even after several weeks. After washing the crystals with ethanol and dichloromethane the yield of **1** was 70% (73 mg). With the crystals being exposed to air, they lose the co-crystallised nitrile molecules.

Analysis (%) for $C_{24}H_{40}N_8Cl_{30}Nb_{12}$, $M = 2619.09\ \text{g} \cdot \text{mol}^{-1}$: calcd. C 11.01, H 1.54, N 4.28; found C 10.83, H, 1.50, N 3.85. – IR (25°C, ATR, 32 Scans, cm^{-1}): $\nu = 558$ (s), 583 (m), 596 (m), 620 (m), 626 (m), 645 (m), 653 (m), 668 (m), 699 (m), 736 (m), 777 (vs), 847 (m), 1004 (w), 1070 (m), 1261 (w), 1306 (m), 1377 (m), 1403 (m), 1455 (m), 2277 (s), 2341 (w), 2361 (w), 2883 (w), 2916 (m), 2945 (m), 2984 (w). – ^{1}H NMR (DMSO-d_6, ppm, r.t.): $\delta = 2.45$ (q. 2 H), 1.15 (t. 3 H).

4.2.3 $[Nb_6Cl_{12}(^nPrCN)_6][Nb_6Cl_{18}] \cdot 2(^nPrCN)$ (2)

The synthesis of the compound was carried out is the same way as for **1**. Instead of propionitrile and acetic anhydride, butyronitrile (^{n}PrCN) and pivalic anhydride ($TMAc_2O$) were used. Using 50 mg of (41.74 µmol) of the precursor compound $[Nb_6Cl_{14}(H_2O)_4] \cdot 4(H_2O)$, **2** was obtained in a yield of 58% (66 mg).

Analysis (%) for $C_{32}H_{56}N_8Cl_{30}Nb_{12}$, $M = 2731.31\ \text{g} \cdot \text{mol}^{-1}$: calcd. C 14.07, H 2.07, N 4.10; found C 13.74, H, 1.87, N 3.83. – IR (25°C, ATR, 32 Scans, cm^{-1}): $\nu = 546$ (m), 701 (m), 732 (vs), 767 (m), 839 (m), 872 (s), 917 (s), 952 (m), 1032 (m), 1055 (m), 1094 (s), 1230 (m), 1253 (m), 1267 (m), 1335 (s), 1383 (m), 1405 (s), 1457 (s), 2281 (vs), 2359 (m), 2875 (m), 2934 (m), 2967 (m). – ^{1}H NMR (DMSO-d_6, ppm, r.t.): $\delta = 2.45$ (t. 2 H), 1.57 (q. 2 H), 0.97 (t. 3 H).

4.2.4 $[Nb_6Cl_{12}(^iPrCN)_6][Nb_6Cl_{18}] \cdot 2\ ^iPrCN$ (3)

The reaction of 20 mg (16.70 µmol) of the precursor $[Nb_6Cl_{14}(H_2O)_4] \cdot 4\,H_2O$ in a mixture of 1 mL of isobutyronitrile (^{i}PrCN) and 1 mL of acetic anhydride (Ac_2O) in a sample glass at 110°C resulted in a dark brown reaction solution. After storage at room temperature for several weeks, large strongly intergrown crystals of **3** were obtained. After purification with dry ethanol and dry dichloromethane, $[Nb_6Cl_{12}(^iPrCN)_6][Nb_6Cl_{18}] \cdot 2(^iPrCN)$ (**3**) was obtained in low yield (29%, 13 mg).

Analysis (no reliable data because too small amounts of substance) – IR (25°C, ATR, 32 Scans, cm^{-1}): $\nu = 490$ (w), 501 (w), 554 (s), 577 (w), 596 (w), 736 (w), 777 (m), 847 (w), 874 (w), 898 (w), 915 (w), 938 (m), 969 (w), 1004 (w), 1047 (w), 1102 (s), 1156 (w), 1173 (m), 1220 (w), 1267 (m), 1313 (m), 1362 (m), 1389 (m), 1455 (s), 1708 (w), 2242 (m), 2275 (vs), 2873 (w), 2897 (w), 2936 (w), 2978 (w). – ^{1}H NMR (DMSO-d_6, ppm, RT): $\delta = 2.87$ (m. 1 H), 1.23 (d. 6 H).

4.3 X-ray structure determinations

All cell measurements as well as the data collection procedures were performed on a Bruker-Nonius Apex D8 diffractometer equipped with a CCD detector and a sealed-tube Mo$K\alpha$ radiation source ($\lambda = 0.71073$ Å). Diffraction measurements were carried out at $T = -150°\text{C}$. The structures were solved by Direct Methods and refined against F^2 by full-matrix least-squares using the program suites by G. M. Sheldrick (vers. 2014-2) [36–39]. All non-hydrogen atoms were refined anisotropically; all hydrogen atoms were placed on geometrically calculated positions and refined by using riding models [38, 39]. The refinements were performed with the aid of SHELXLE as graphical interface [40]. The illustrations of the structures were generated with the program DIAMOND 4 [41].

CCDC 1817708 (**1**), 1817680 (**2**), and 1896965 (**3**) contain the supplementary crystallographic data for this paper. These data can be obtained free of charge from The Cambridge Crystallographic Data Centre *via* www.ccdc.cam.ac.uk/data_request/cif.

References

[1] A. Simon, *Angew. Chem., Int. Ed. Engl.* **1981**, *20*, 1–22.
[2] A. Simon, *Angew. Chem., Int. Ed. Engl.* **1988**, *27*, 159–183.
[3] R. W. Berg, *Coord. Chem. Rev.* **1992**, *113*, 1–130.
[4] P. Braunstein, L. A. Oro, P. R. Raithby (Eds.), *Metal Clusters in Chemistry*, Wiley-VCH, Weinheim **1999**.
[5] T. Hughbanks, *J. Alloys Compd.* **1995**, *229*, 40–53.
[6] P. Lemoine, J.-F. Halet, S. Cordier, in *Ligated Transition Metal Clusters in Solid-State Chemistry: The legacy of Marcel Sergent* (Ed.: J.-F. Halet), *Structure and Bonding*, Vol. 180, (Series ed.: D. M. P. Mingos), Springer International Publishing, Cham, **2019**, pp. 143–190.

[7] E. V. Anokhina, A. Lachgar, in *Inorganic Chemistry in Focus III*, (Eds.: G. Meyer, D. Naumann, L. Wesemann), Wiley-VCH, Weinheim, **2006**, pp. 79–104.

[8] A. Simon, *Phil. Trans. R. Soc., A* **2010**, *368*, 1285–1299.

[9] G. Svensson, J. Köhler, A. Simon, in *Metal Clusters in Chemistry* (Eds.: P. Braunstein, L. A. Oro, P. R. Raithby), Wiley-VCH, Weinheim **1999**, pp. 1509–1550.

[10] O. Reckeweg, H.-J. Meyer, *Z. Naturforsch.* **1995**, *50b*, 1377–1381.

[11] A. Flemming, J. König, M. Köckerling, *Z. Anorg. Allg. Chem.* **2013**, *639*, 2527–2531.

[12] H. Imoto, S. Hayakawa, N. Morita, T. Saito, *Inorg. Chem.* **1990**, *29*, 2007–2014.

[13] E. Sperlich, M. Köckerling, *Z. Naturforsch.* **2019**, *74b*, 751–755.

[14] T. G. Gray, *Coord. Chem. Rev.* **2003**, *243*, 213–235.

[15] F. Ogliaro, S. Cordier, J.-F. Halet, C. Perrin, J.-Y. Saillard, M. Sergent, *Inorg. Chem.* **1998**, *37*, 6199–6207.

[16] T. Hughbanks, *Prog. Solid State Chem.* **1989**, *19*, 329–372.

[17] R. Eisenbraun, H. Schäfer, *Z. Anorg. Allg. Chem.* **1985**, *530*, 222–226.

[18] J. Espenson, N. E. Cooke, T. Kuwana, *Inorg. Chem.* **1971**, *10*, 1081–1083.

[19] I. Bašic, N. Brničević, U. Beck, A. Simon, R. E. McCarley, *Z. Anorg. Allg. Chem.* **1998**, *624*, 725–732.

[20] N. Brničević, S. Širac, I. Bašic, Z. Zhang, R. E. McCarley, I. A. Guzei, *Inorg. Chem.* **1999**, *38*, 4159–4162.

[21] P. Planinić, V. Rastija, B. Perić, G. Giester, N. Brničević, *C. R. Chim.* **2005**, *8*, 1766–1773.

[22] E. S. Bosch, M. Köckerling, *Comments Inorg. Chem.* **2009**, *30*, 119–129.

[23] S. Širac, P. Planinić, L. Marić, N. Brničević, R. E. McCarley, *Inorg. Chim. Acta* **1998**, *271*, 239–242.

[24] J. E. Land, H. H. Musgrove, J. E. Teggins, *J. Less Common Met.* **1971**, *23*, 307–312.

[25] H. Schäfer, H. Plautz, H. Baumann, *Z. Anorg. Allg. Chem.* **1973**, *401*, 63–84.

[26] A. Simon, H.-G. von Schnering, H. Schäfer, *Z. Anorg. Allg. Chem.* **1968**, *361*, 235–248.

[27] H. W. Rohm, M. Köckerling, *Z. Anorg. Allg. Chem.* **2003**, *629*, 2356–2362.

[28] J. Zhang, J. D. Corbett, *Inorg. Chem.* **1995**, *34*, 1652–1656.

[29] F. W. Koknat, R. E. McCarley, *Inorg. Chem.* **1972**, *11*, 812–816.

[30] J. König, I. Dartsch, A. Topp, E. Guillamón, R. Llusar, M. Köckerling, *Z. Anorg. Allg. Chem.* **2016**, *642*, 572–578.

[31] P. A. Wood, S. J. Borwick, D. J. Watkin, W. D. S. Motherwell, F. H. Allen, *Acta Crystallogr.* **2008**, *B64*, 393–396.

[32] R. A. Nyquist (Ed.), *Interpreting Infrared, Raman, and Nuclear Magnetic Resonance Spectra*, Academic Press, Cambridge, MA (USA) **2001**.

[33] J. Reedijk, A. P. Zuur, W. L. Groeneveld, *Recl. Trav. Chim. Pays-Bas* **1967**, *86*, 1127–1137.

[34] P. Planinić, V. Rastija, S. Širac, M. Vojnović, L. Frkanec, N. Brničević, R. E. McCarley, *J. Clust. Sci.* **2002**, *13*, 215–222.

[35] F. W. Koknat, J. A. Parson, A. Vongvusharintra, *Inorg. Chem.* **1974**, *13*, 1699–1702.

[36] G. M. Sheldrick, SHELXS/L, Programs for Crystal Structure Determination, University of Göttingen, Göttingen (Germany) **2014**.

[37] G. Sheldrick, *Acta Crystallogr.* **1990**, *A46*, 467–473.

[38] G. M. Sheldrick, *Acta Crystallogr.* **2008**, *A64*, 112–122.

[39] G. M. Sheldrick, *Acta Crystallogr.* **2015**, *C71*, 3–8.

[40] C. B. Hübschle, G. M. Sheldrick, B. Dittrich, *J. Appl. Crystallogr.* **2011**, *44*, 1281–1284.

[41] G. Bergerhoff, M. Berndt, K. Brandenburg, *J. Res. Natl. Inst. Stand. Technol.* **1996**, *101*, 221–225.